PERGAMON

International Journal of Multiphase Flow 25 (1999) 395–410

International Journal of Multiphase Flow

Gas–liquid two-phase flow in microchannels Part II: void fraction and pressure drop

K.A. Triplett, S.M. Ghiaasiaan *, S.I. Abdel-Khalik, A. LeMouel, B.N. McCord

G. W. Woodruff School of Mechanical Engineering, Georgia Institute of Technology, Atlanta, GA 30332-0405, USA

Received 16 December 1997; received in revised form 18 August 1998

Abstract

Void fraction and two-phase frictional pressure drop in microchannels were experimentally investigated. Using air and water, experiments were conducted in transparent circular microchannels with 1.1 and 1.45 mm inner diameters and in microchannels with semi-triangular (triangular with one corner smoothed) cross-sections with hydraulic diameters 1.09 and 1.49 mm. Gas and liquid superficial velocities were varied in the 0.02–80 m/s and 0.02–8 m/s ranges, respectively, and void fractions were calculated by analyzing photographs taken from the test sections with circular cross-section.

Measured void fractions were compared with several correlations. The homogeneous flow model provided the best prediction of the experimental void fractions in bubbly and slug flow patterns. The homogeneous flow model and all other tested empirical correlations significantly over predicted the void fractions in annular flow pattern, however.

A one-dimensional model, based on the numerical solution of mass and momentum conservation equations was applied for the calculation of test section pressure drops, using various two-phase friction models. For bubbly and slug flow patterns, the two-phase friction factor based on homogeneous mixture assumption provided the best agreement with experimental data. For annular flow the homogeneous mixture model and other widely used correlations significantly over predicted the frictional pressure drop. © 1999 Elsevier Science Ltd. All rights reserved.

Keywords: Microchannels; Two-phase flow; Friction; Pressure drop; Flow patterns; Void fraction; Hold-up

* Corresponding author. Fax: 001 404 894 3733.

PII: S0301-9322(98)00055-X

1. Introduction

The objective of this investigation was to systematically study the gas–liquid two-phase flow patterns, void fraction and pressure drop in capillaries with circular cross-sections and capillaries representing the flow channels in rod bundles with small, triangular-pitched arrays. In part I of this paper (Triplett et al., 1999) the experimental results dealing with two-phase flow patterns were presented and discussed. The experimental void fraction and two-phase pressure drop results are presented in this (part II) article.

2. Background

Various aspects of two-phase flow and change-of-phase heat transfer in microchannels have been investigated recently, including two-phase critical flow (Narabayashi and Makoto et al., 1991; John et al., 1988; Ghiaasiaan et al., 1997), two-phase flow patterns (Damianides and Westwater, 1988; Fukano and Kariyasaki, 1993; Triplett et al., 1999), and two-phase pressure drop (Inasaka et al., 1989; Fukano and Kariyasaki, 1993; Bao et al., 1994; Fourar and Bories, 1995). These investigations, in general, indicate that two-phase flow hydrodynamics in microchannels are different from the hydrodynamics in larger channels. With respect to flow patterns, for example, due to the dominance of surface tension, stratified flow is essentially absent, slug (plug) and churn flow patterns occur over extensive parameter ranges, and, at least in the latter two flow patterns, velocity slip is small (Fukano and Kariyasaki, 1993; Triplett et al., 1999).

Pressure drop and void fraction (gas hold-up) are among the most important hydrodynamic aspects of two-phase flow. Two-phase pressure drop in channels in particular is an essential element for the design of piping and process systems, and has been the subject of numerous experimental studies and a large number of empirical and semi-analytical predictive methods. The most widely-used correlations, in spite of the basic theoretical arguments leading to their development (which may assume particular flow patterns, often annular), are presented as flow regime-independent correlations for obvious practical reasons (Lockhart and Martinelli, 1949; Chisholm, 1973; Baroczy, 1965; Beattie and Whalley, 1982; Friedel, 1979). Examples to the point are the correlations of Friedel (1979) which are empirical fits to some 15,000 data points for vertical flow and 10,000 data points for horizontal flow. Nevertheless, these correlations may perform poorly when applied to high void fraction annular flow (Yao and Ghiaasiaan, 1996). Furthermore, the bulk of the previously generated data and the previously-published predictive methods represent two-phase flow in channels several mm in diameter or larger.

The objective of this work is to experimentally study frictional pressure drop and void fraction associated with gas–liquid two-phase flow in microchannels. Horizontal, circular channels with 1.1 and 1.45 mm inner diameters, and semi-triangular channels with 1.09 and 1.49 mm hydraulic diameters, with air and water, are used. Based on the generated data the adequacy of the existing widely-used predictive methods for application to microchannels is examined.

3. Experiments

3.1. Apparatus

Experiments were performed using the test facility and instruments described in part I of this paper (Triplett et al., 1999). Therefore, only the experimental attributes directly dealing with pressure drop and void fraction measurements are briefly discussed here.

Two differential pressure transducers are used to measure the pressure drop in the channel and the pressure drop associated with the channel exit. A differential pressure transducer labeled 7a in Fig. 1 of Triplett et al. (1999) measures the static pressure drop along an approximately 20 cm-long segment of the channel. The length of this segment varied slightly with each test section and was 200, 195, 192 and 193 mm, respectively, for test sections (a–d). The second differential pressure transducer, labeled 7b in Fig. 1 of Triplett et al. (1999), measures the pressure difference between a pressure tap on test section to which the aforementioned differential pressure transducer is connected, and the channel exit. The channel exit was always open to a chamber at atmospheric pressure. Both pressure transducers (Rosemount, Model 1151 DP5E22) had a differential pressure range of 0–186.8 kPa, and an accuracy of ± 0.4 kPa. The pressure transducers were calibrated using the laboratory's building air supply and a pre-calibrated pressure gauge.

3.2. Procedures

In the experiments, after the system was leak tested (as described in Triplett et al., 1998), a check was performed to ensure that the pressure transducers and their inlet lines were filled with water. This was done by first imposing a steady, high flow rate of water through the system and then blocking the end of the test section. The water flowing backwards due to the blockage of the channels would flow through the transducer connecting lines and displace trapped air, which was then removed through bleed valves. This procedure was continued, until the bleed lines were visibly clear of any air pocket.

In the experiments, liquid (tap water at room temperature) and air volume flow rates are set at desired levels first, and after steady-state is established 10 pressure drop measurements are recorded, and their average is calculated and used. The centers of the test sections were photographed. The photographs were used for flow pattern identification (Triplett et al., 1999) and for the estimation of channel average void fraction for circular test sections [test sections (a) and (b), as described below].

3.3. Void fraction measurement

Void fractions were estimated by analyzing photographs taken from the center of the test section. Each photograph typically covered a 6 mm-long segment of the test section.

In the bubbly flow pattern, individual bubbles were assumed to be spheres or ellipsoidals, depending on their shape. In slug flow, the Taylor bubbles were divided into cylinders and spherical segments. In bubbly flow each photo typically covered a large number of bubbles, thus providing a reasonable volume-averaged estimate of the void fraction. In slug flow the

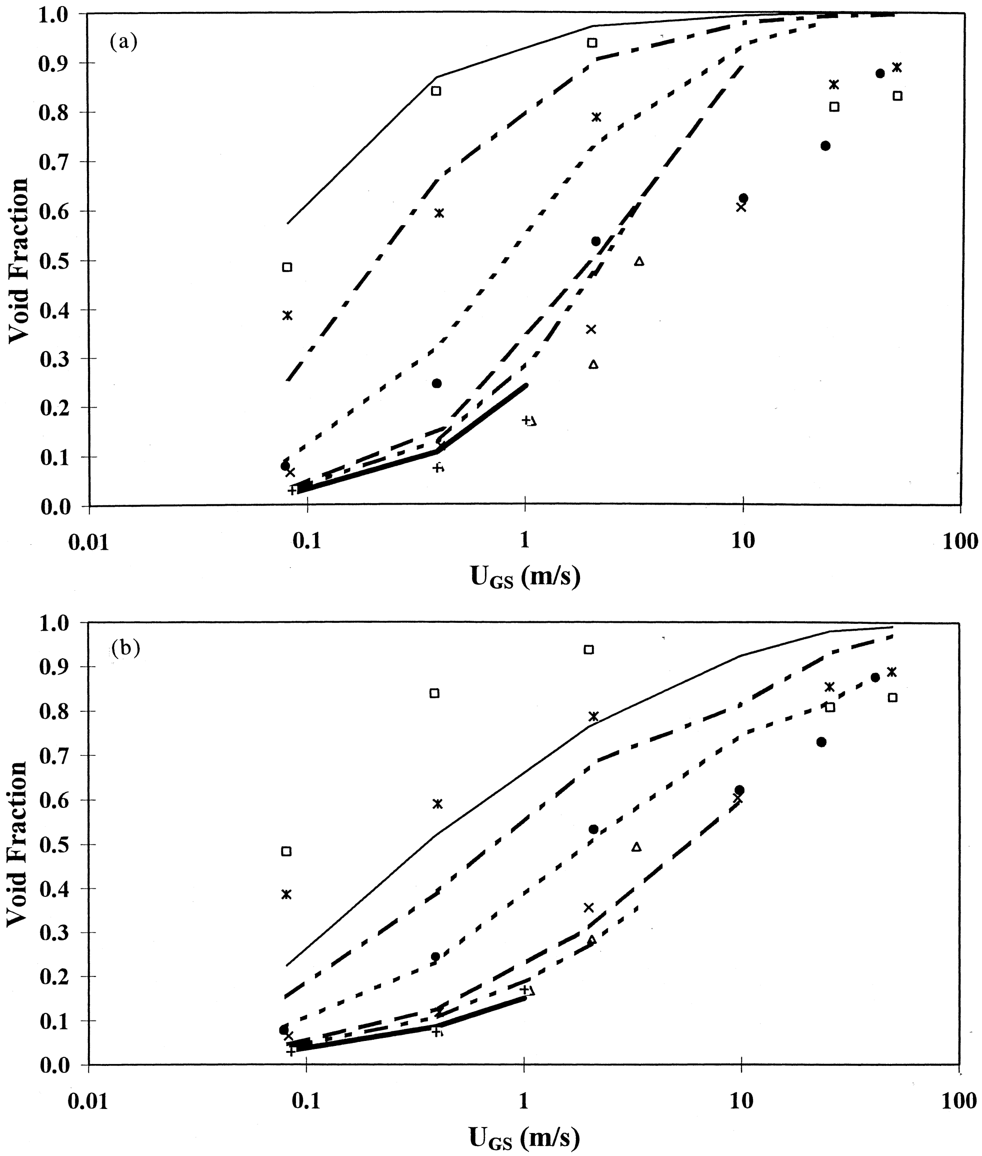

Fig. 1. Comparison of measured void fractions with predictions of various correlations for test section (a): (a) homogeneous flow model; (b) Chexal et al. (1997); (c) Lockhart–Martinelli–Butterworth (Butterworth, 1975); (d) CISE (Premoli, 1971).

flow pattern is relatively regular and average Taylor bubble and liquid slug lengths were calculated from multiple photos and used for void fraction calculation.

In the annular flow pattern the vapor core was divided into several cylinders and the channel average void fraction was calculated accordingly. Slug-annular and churn flow patterns were the most difficult flow regimes to analyze. The void fractions associated with slug-annular flow

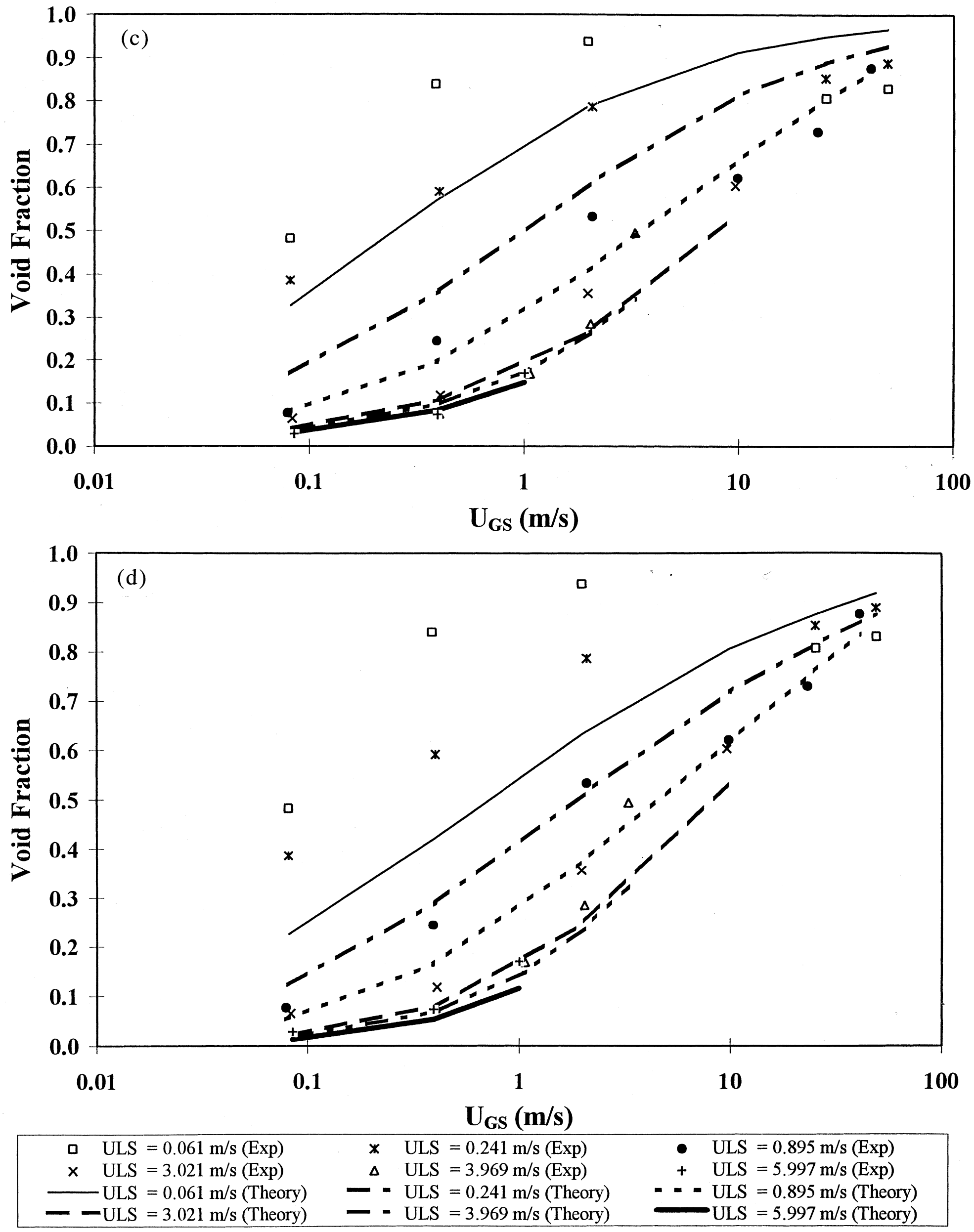

Fig. 1 (*Continued*)

patterns are not included in the analysis due to their high uncertainty. In churn flow, an average of 0.5 local void fraction was assumed in segments of the flow field where the gas phase was dispersed.

3.4. Measurement uncertainties

Detailed error analyses in which the uncertainties in measured channel dimensions and measurements made by instruments were considered, led to the following estimated maximum uncertainties: 7.5% for liquid superficial velocity, 5.5% for gas superficial velocity, and 10% for pressure drop measurements when the measured pressure drop was larger than 2.0 kPa.

Estimation of the uncertainty associated with the void fractions is difficult. Repetition of the void fraction calculations for a typical photo, where the volume of the gaseous pockets were assigned their apparent maximum and minimum magnitudes, typically led to about 10% change in the calculated channel void fraction. Repetition of calculations using different photos taken from selected tests also typically led to less than 10% difference in the calculated void fractions. A reasonable estimate for the uncertainty limit on the depicted void fractions is thus about $\pm 15\%$ (i.e. true α is likely to be between 0.85 and 1.15 times the measured α).

4. Theoretical considerations

4.1. Method of analysis of pressure drop data

All the experiments were performed with air and water in microchannels with very large aspect ratios. Therefore, it is assumed that the flow field is one-dimensional (1-D) and steady-state. It is also assumed that the liquid is impermeable to gas. Since the contribution of water vapor to the gas phase is everywhere negligible, the gas is assumed to be pure air and act as an ideal gas. Details of two-phase flow patterns and their associated flow pattern-dependent interfacial momentum transfer processes are not well-understood for microchannels, therefore separate phasic momentum conservation equations will not be applied, and instead the gas–liquid mechanical nonequilibrium is represented by a slip ratio, S, defined as:

$$S = U_G/U_L \tag{1}$$

where U_G and U_L are the gas and liquid phasic velocities, respectively.

The liquid and gas-phase mass conservation and the two-phase mixture momentum conservation equations are considered. When the slip ratio, S, and the two-phase frictional pressure gradient, $(-\mathrm{d}P/\mathrm{d}z)_{F,TP}$, are represented by algebraic relations in terms of void fraction, α (or x, the quality), liquid velocity, U_L, and pressure P properties, the conservation equations will include three unknowns, α, U_L and P. Using appropriate thermodynamic relations, these equations are expanded (Ghiaasiaan et al., 1995), and the following equation is derived:

$$\mathbf{A}\frac{\mathrm{d}\mathbf{Y}}{\mathrm{d}z} = \mathbf{C} \tag{2}$$

where $\mathbf{A}$ is a 3×3 coefficient matrix, $\mathbf{C}$ is a three-dimensional column vector, and the column vector $\mathbf{Y}$ is defined as:

$$\mathbf{Y} = (P, \alpha, U_L)^T \tag{3}$$

where superscript T implies transpose.

In model calculations, the set of ordinary differential equations represented by Eq. (2) are numerically integrated using the fourth-order Runge–Kutta technique. Numerical calculations are performed by guessing the pressure at channel inlet, $z = 0$, and integrating the above ordinary differential equations up to the exit of the test section. The solution is repeated iteratively, with P at $z = 0$ as the iteration parameter, until the calculated pressure corresponding to the channel exit becomes equal to the experimental (atmospheric) pressure.

4.2. Void fraction and slip ratio correlations

Empirical void fraction correlations, relating α to the Martinelli factor, X and from there to quality, x, have been provided by Lockhart and Martinelli (1949), Baroczy (1963), and Wallis (1969), and have been discussed by Butterworth (1975) and Chen and Spedding (1983). Butterworth (1975) showed that Lockhart and Martinelli's correlation for void fraction, as well as several other void fraction correlations, can be represented in the following generic form:

$$\frac{1-\alpha}{\alpha} = A\left(\frac{1-x}{x}\right)^p \left(\frac{\rho_G}{\rho_L}\right)^q \left(\frac{\mu_L}{\mu_G}\right)^r \tag{4}$$

where $A = 0.28$, $p = 0.64$, $q = 0.36$ and $r = 0.07$ for Lockhart and Martinelli, and $A = 1$, $p = 0.74$, $q = 0.65$ and $r = 0.13$ for a correlation due to Baroczy (1963).

A correlation for the slip ratio, S, derived by the CISE group (Premoli et al., 1971; Hewitt, 1983), can be represented as

$$S = 1 + B_1\left(\frac{y}{1 + yB_2} - yB_2\right)^{1/2} \tag{5}$$

where $y = (1-\beta)/\beta$, and

$$\beta = U_G\alpha/[U_G\alpha + U_L(1-\alpha)], \tag{6}$$

$$B_1 = 1.578 Re_{L0}^{-0.19}(\rho_L/\rho_G)^{0.22}, \tag{7}$$

$$B_2 = 0.0273 We_{L0} Re_{L0}^{-0.51}(\rho_L/\rho_G)^{-0.08}, \tag{8}$$

$$Re_{L0} = GD/\mu_L, \tag{9}$$

$$We_{L0} = G^2 D/(\sigma\rho_L). \tag{10}$$

In the above equations D represents the channel diameter, σ is the surface tension, μ_L is the dynamic viscosity of the liquid, and Re_{L0} and We_{L0} represent Reynolds and Weber numbers, respectively, when all fluid is liquid. Bao et al. (1994) compared the above correlation with their microchannel void fraction data, with relatively good agreement.

Chexal et al. (1997) have developed a versatile correlation for void fraction in 1-D two-phase flow in channels. The correlation, which is based on the drift flux model (Zuber and Findlay, 1965), has been refined and improved in order to expand its range of validity (Chexal and Lellouche, 1986; Chexal et al., 1992, 1997).

4.3. Frictional pressure drop correlations

The homogeneous mixture model is the simplest method for calculating the frictional two-phase pressure drop, and has been found by Ungar and Cornwell (1992) to reasonably agree with their experimental data representing the flow of two-phase ammonia in microchannels with $D = 1.46$–3.15 mm. Accordingly:

$$\left(\frac{-\mathrm{d}P}{\mathrm{d}z}\right)_{\mathrm{F,TP}} = f_{\mathrm{TP}}\frac{1}{D}\frac{2G^2}{\rho_{\mathrm{TP}}} \tag{11}$$

where f_{TP} and ρ_{TP} represent the two-phase Fanning friction factor and density, respectively. The friction factor is assumed to depend on the two-phase Reynolds number according to Blasius's correlation for turbulent flow where (McAdams, 1954):

$$Re_{\mathrm{TP}} = \frac{GD}{\mu_{\mathrm{TP}}} \tag{12}$$

where ρ_{TP} is the homogeneous mixture density, and

$$\mu_{\mathrm{TP}} = \left(\frac{x}{\mu_{\mathrm{G}}} + \frac{1-x}{\mu_{\mathrm{L}}}\right)^{-1}. \tag{13}$$

Based on an extensive experimental data bank, Friedel (1979) derived the following correlation for the all-liquid two-phase flow multiplier in horizontal channels:

$$\Phi_{\mathrm{L0}}^2 = A + 3.24x^{0.78}(1-x)^{0.224}\left(\frac{\rho_{\mathrm{L}}}{\rho_{\mathrm{L}}}\right)^{0.91}\left(\frac{\mu_{\mathrm{G}}}{\mu_{\mathrm{L}}}\right)^{0.19}\left(1-\frac{\mu_{\mathrm{G}}}{\mu_{\mathrm{L}}}\right)^{0.7} Fr_{\mathrm{TP}}^{-0.0454}We_{\mathrm{TP}}^{-0.035} \tag{14}$$

where

$$A = (1-x)^2 + x^2\rho_{\mathrm{L}}f_{\mathrm{G0}}(\rho_{\mathrm{G}}f_{\mathrm{L0}})^{-1}. \tag{15}$$

The two-phase Froude and Weber numbers are defined, respectively, as:

$$Fr_{\mathrm{TP}} = \frac{G^2}{gD\rho_{\mathrm{TP}}^2}, \tag{16}$$

$$We_{\mathrm{TP}} = \frac{G^2D}{\sigma\rho_{\mathrm{TP}}}. \tag{17}$$

The single-phase friction factors are obtained, for $j = L$ and G, as follows. Define the phasic Reynolds numbers as:

$$Re_j = DG/\mu_j. \quad (18)$$

When $Re_j \leqslant 1055$, $f_{j0} = 16/Re_j$. When $Re_j > 1055$:

$$f_{j0} = 0.25[0.86859 \ln\{Re_j/(1.964 \ln Re_j - 3.8215)\}]^{-2}. \quad (19)$$

Using Eq. (14), the two-phase frictional pressure gradient is obtained from:

$$(-\mathrm{d}P/\mathrm{d}z)_{\mathrm{F,TP}} = \Phi^2_{\mathrm{L0}}(-\mathrm{d}P/\mathrm{d}z)_{\mathrm{F,LO}} \quad (20)$$

where $(-\mathrm{d}P/\mathrm{d}z)_{\mathrm{F,L0}}$ represents the frictional pressure gradient when all fluid is assumed to be liquid.

5. Results and discussion

5.1. Void fraction

The estimated experimental void fractions for test section (a) are compared with predictions of the homogeneous flow model and the empirical correlations summarized earlier in Fig. 1 (a)–(d). Similar comparisons, representing test section (b), are depicted in Fig. 2 (a), (b). Data and correlation predictions all represent the test section centers. Overall, α monatomically increases with increasing gas superficial velocity, U_{GS}, for constant liquid superficial velocity, U_{LS}, and decreases with increasing U_{LS} for constant U_{GS}. The apparent deviations from the aforementioned trends are likely to be due to the difficulty, and the larger uncertainty, associated with the calculation of void fractions using photographs.

Fig. 1 (a) and 2 (a) indicate that the homogeneous flow model provides a satisfactory prediction of the channel void fractions at low U_{GS} values, corresponding to bubbly and slug two-phase flow patterns. For churn and annular flow patterns, where relatively significant interphase slip is likely due to the separation of the liquid and gas phases, the homogeneous flow model evidently over predicts the experimental data by large margins.

The agreement between the experimental data and the correlation of Chexal et al. (1997), as noted in Fig. 1 (b) and 2 (b), is good for bubbly and slug flow patterns and at high U_{LS} values and is comparable with the predictions of the homogeneous model. At lower U_{LS} values, however, the correlation of Chexal et al. appears to underestimate the void fractions, likely due to an over prediction of the velocity slip ratio. The latter correlation, furthermore, appears to over predict the void fractions in churn and annular flow patterns systematically and significantly, although with margins notably smaller than the over prediction margins associated with the homogeneous model.

The predictions of the Lockhart–Martinelli–Butterworth correlation (4) (Butterworth, 1975) and the CISE correlation (5) (Premoli et al., 1971), are compared with the void fraction data in Fig. 1 (c) and (d) for test section (a). The predictions of Butterworth's (1975) representation of Baroczy's correlation (Baroczy, 1963) are not depicted for brevity. Overall, however, Baroczy's correlation did not appear to be significantly different than Eq. (4). The correlations of Butterworth (4), and CISE (5), both well-predict α in bubbly and slug flow patterns

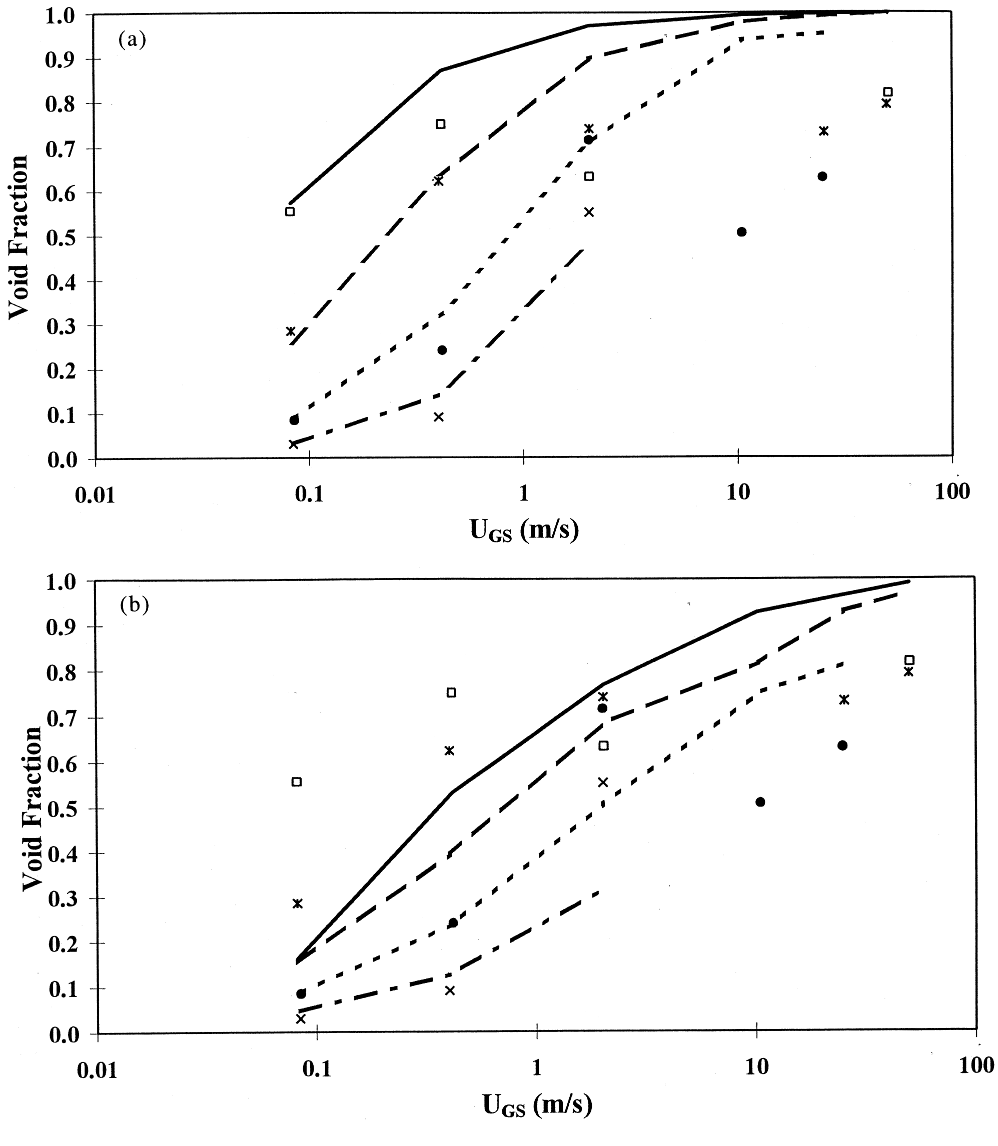

Fig. 2. Comparison of measured void fractions with predictions of various correlations for test section (b): (a) homogeneous flow model; (b) Chexal et al. (1997).

representing high U_{LS} values, and they both over predict α for churn and annular flow patterns.

The results depicted in Figs. 1 and 2 thus indicate that, among the correlations examined in this study, for bubbly and slug flow patterns, the homogeneous flow model overall provides the most accurate prediction of the channel void fraction. Other correlations, however, all satisfactorily agreed with data for the latter flow patterns, except when U_{LS} was very low where the latter correlations significantly under predicted the measured void fractions. This under prediction of α is likely to be due to the differences between two-phase flow patterns in large channels and capillaries. The tested empirical correlations, which are predominantly based on experimental data obtained with large channels, by under predicting void fractions at low U_{LS} in fact account for significant interphase velocity slip which must occur in large channels subject to the same gas and liquid superficial velocities. Such velocity slips are evidently absent in microchannel experiments.

Figs. 1 and 2, furthermore, indicate that all tested methods over predict the void fraction in annular flow. The latter over prediction for homogeneous flow model is of course expected. The apparent systematic over prediction of α in annular flow pattern by the tested correlations indicates lower interphase slip in microchannels in comparison with large channels, and indicates that gas–liquid interfacial friction phenomena in large and microchannels may be significantly different.

5.2. Pressure drop

Fig. 3 (a), (b) and (c) depict typical measured pressure drops over the 200, 195, and 192 mm-long segments of test sections (a), (b) and (c), respectively, as functions of the liquid and gas superficial velocities, U_{LS} and U_{GS}. Model predictions obtained from the numerical solution of the set of ordinary differential equations represented by Eq. (2) assuming equal phasic velocities (homogeneous flow model), and using Eqs. (11–13) (referred to hereafter as the homogeneous pressure drop model), are also depicted in the figures. Note that the total static pressure drops (including frictional pressure loss and pressure drop due to acceleration resulting from the volumetric expansion of air) are shown in these figures.

The predicted pressure drops, obtained with a homogeneous pressure drop model, everywhere normalized with corresponding experimentally-measured pressure drops, are displayed in Fig. 4 for test section (a) where the channel two-phase flow patterns are also specified. Overall, the homogeneous pressure drop model, as expected, well predicts the experimental data in bubbly and slug flow patterns and at high Re_L (where $Re_L = \rho_L U_{LS} D/\mu_L$), where the homogeneous flow assumption is well applicable. Relatively significant deviations are mostly associated with slug-annular and annular flow patterns, and slug flow at very low Re_L.

Fig. 5 displays model-predicted pressure drops, everywhere normalized with experimentally measured pressure drops for test section (d). The model predictions in this figure were obtained by using the homogeneous flow (no slip) assumption, and using Friedel's correlation (Friedel, 1979), (14–20), for two-phase wall friction. Once again model predictions are in satisfactory agreement with data for bubbly and slug flow patterns at high Re_L. They, however, deviate from experimental data rather significantly at low Re_L values. Compared with the homogeneous two-phase frictional pressure drop model, Friedel's correlation evidently provides less accurate predictions for the experimental data.

The acceleration pressure drop in microchannels can be significant due to the very large total pressure drops which result in significant gas density variations in the channel. Typical total and acceleration pressure drops are depicted in Fig. 6 for test section (a), where the displayed total pressure drops represent the measured values and the acceleration pressure drops have been calculated assuming homogeneous flow. As noted, the acceleration pressure drops were significant for tests with high liquid and gas superficial velocities.

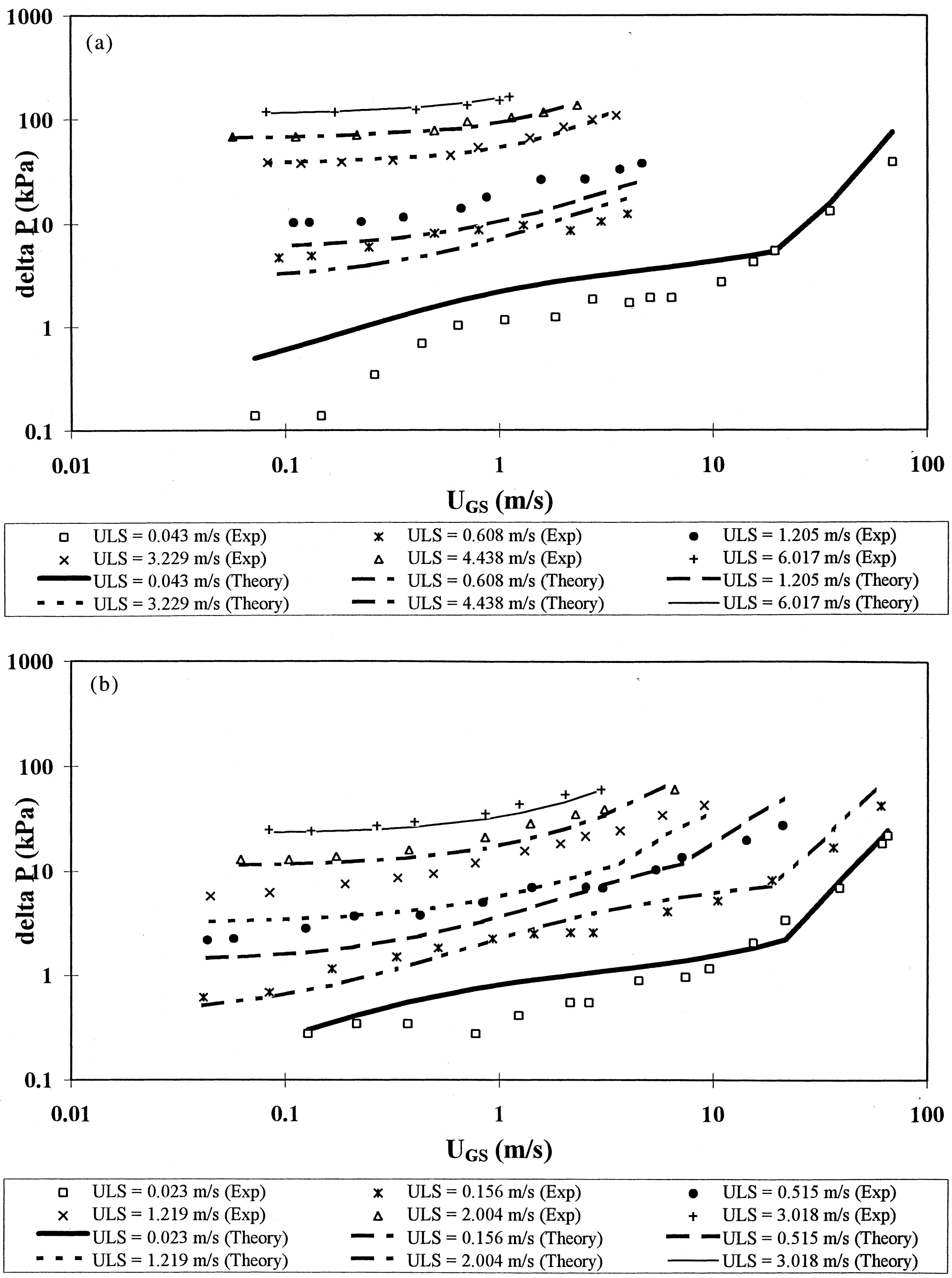

Fig. 3. Typical measured and predicted pressure drops over the test sections. (Model predictions represent homogeneous wall friction model): (a) test section (a); (b) test section (b); (c) test section (c).

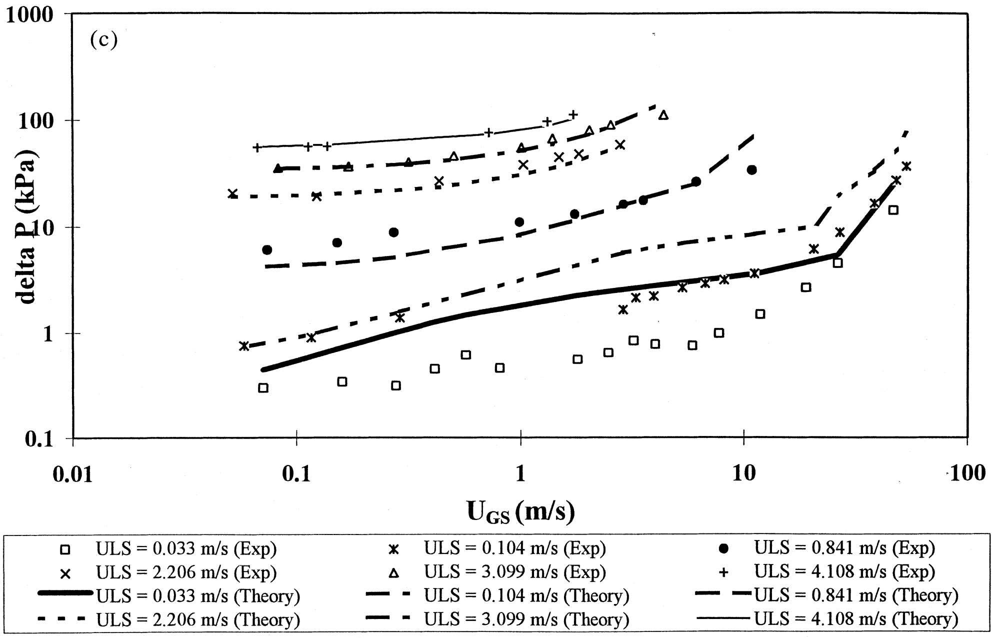

Fig. 3 (*Continued*)

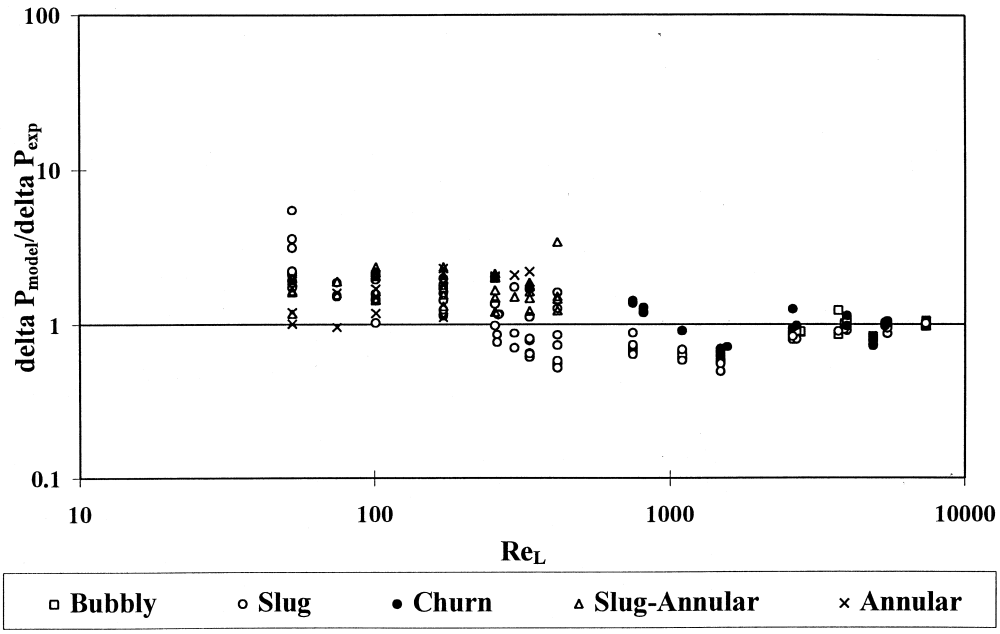

Fig. 4. Model-predicted pressure drops normalized with experimentally-measured pressure drops for test section (a). (Model predictions represent homogeneous wall friction model).

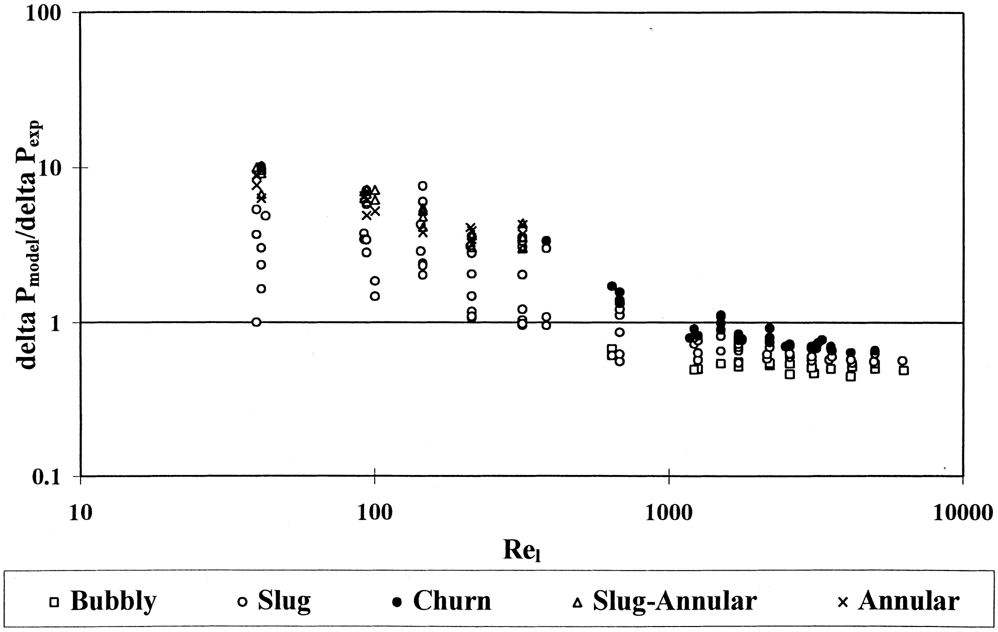

Fig. 5. Model-predicted pressure drops normalized with experimentally-measured pressure drops for test section (d). (Model predictions represent Friedel's (1979) correlation).

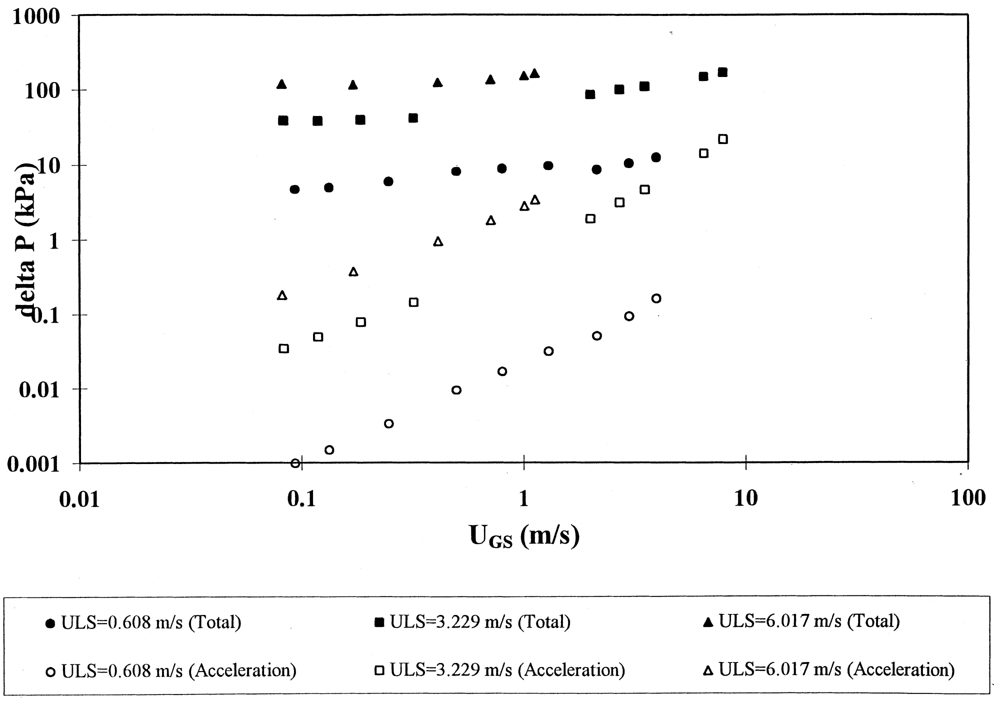

Fig. 6. Typical total and acceleration pressure drops for test section (a).

In summary, the results of this study indicate that among the widely-used methods for calculating the void fraction and frictional pressure drop in adiabatic two-phase channel flow, the homogeneous two-phase flow (zero slip) and homogeneous pressure drop models provide the best predictions for microchannels. The homogeneous flow model, as well as other widely-used empirical correlations for interphase slip and wall friction, however, do not predict the void fraction and frictional pressure drop in annular flow with accuracy, indicating the need for further experimental and analytical study of annular flow in microchannels.

6. Concluding remarks

Void fraction and two-phase pressure drop were measured in transparent long horizontal microchannels with circular and semi-triangular (triangular with one corner smoothed) cross-sections. The test section hydraulic diameters were 1.1 and 1.45 mm for circular channels, and 1.09 and 1.49 mm for semi-triangular cross-section test sections. The gas and liquid superficial velocities were varied in the 0.02–80 m/s and 0.02–8 m/s ranges, respectively. Flow patterns were discussed in part I of this paper.

Measured void fractions were compared with predictions of the homogeneous mixture model, the correlation of Butterworth (1975) representing the empirical correlation of Lockhart and Martinelli (1949), the CISE correlation (Premoli et al., 1971), and the correlation of Chexal et al. (1997). A one-dimensional model based on the numerical solution of mass and momentum conservation equations was used for calculating the channel pressure drops utilizing various two-phase friction models. The two-phase friction factors based on the homogeneous mixture assumption and the empirical correlations of Chisholm (1973) and Friedel (1979) were examined.

Void fraction and channel pressure drop were best predicted by the homogeneous mixture assumption. The tested models and correlations all over predicted the channel void fraction and pressure drop in the annular flow pattern, suggesting that the annular flow liquid–gas interfacial momentum transfer and wall friction in microchannels may be significantly different from similar processes in larger channels. Systematic experiments addressing the hydrodynamics of the annular flow pattern in microchannels are thus recommended.

References

Bao, Z.Y., Bosnick, M.G., Haynes, B.S., 1994. Estimation of void fraction and pressure drop for two-phase flow in fine passages. Trans. Inst. Chem. Eng. 72, 625–632.

Baroczy, C.J., 1963. Correlation of liquid fraction in two-phase flow with application to liquid metals, NAA-SR-8171. Butterworth, London, 1975.

Baroczy, C.J. 1965. A systematic correlation for two-phase pressure drop, presented at 8th National Heat Transfer Conference. Los Angeles, CA. American Society of Mechanical Engineers, New York.

Beattie, D.R.H., Whalley, P.B., 1982. A simple two-phase frictional pressure drop calculation method. Int. J. Multiphase Flow 8, 83–89.

Butterworth, D., 1975. A comparison of some void-fraction relationships for co-current gas–liquid flow. Int. J. Multiphase Flow 1, 845–850.

Chen, J.J.J., Spedding, P.L., 1983. An analysis of holdup in horizontal two-phase gas–liquid flow. Int. J. Multiphase Flow 9, 147–159.

Chexal, B., Lellouche, G.S., 1986. A full range drift-flux correlation for vertical flow. Electric Power Research Institute report EPRI-NP-3989-SR (revision 1). Palo Alto, CA.

Chexal, B., Lellouche, G.S., Horowitz, J., Healzer, J., 1992. A void fraction correlation for generalized applications. Prog. Nucl. Energy 27, 255–295.

Chexal, B., Merilo, M., Maulbetsch, J., Horowitz, J., Harrison, J., Westacott, J.C., Peterson, C., Kastner, W., Schmidt, H., 1997. Void fraction technology for design and analysis. Electric Power Research Institute. Palo Alto, CA.

Chisholm, D.A., 1973. Pressure gradients due to friction during the flow of evaporating two-phase mixture in smooth tubes and channels. Int. J. Heat Mass Transfer 16, 347–358.

Damianides, C.A., Westwater, J.W., 1988. Two-phase flow patterns in a compact heat exchanger and in small tubes. Proceedings of the Second UK National Conf. On Heat Transfer. Glasgow, 14–16 September. Mechanical Engineering Publications, London, pp. 1257–1268.

Fourar, M., Bories, S., 1995. Experimental study of air–water two-phase flow through a fracture (narrow channel). Int. J. Multiphase Flow 21, 621–637.

Friedel, L., 1979. Improved friction pressure drop correlations for horizontal and vertical two-phase pipe flow. 3R International, 18 Jahngrang, Hef 7.

Fukano, T., Kariyasaki, A., 1993. Characteristics of gas–liquid two-phase flow in a capillary. Nucl. Eng. Des. 141, 59–68.

Ghiaasiaan, S.M., Kamboj, B.K., Abdel-Khalik, S.I., 1995. Two-fluid modeling of condensation in the presence of non-condensables in two-phase channel flow. Nucl. Sci. Eng. 119, 1–17.

Ghiaasiaan, S.M., Muller, J.R., Sadowski, D.L., Abdel-Khalik, S.I., 1997. Critical flow of initially highly subcooled water through a short capillary. Nucl. Sci. Eng. 126, 229–238.

Hewitt, G.F., 1983. Gas–liquid flow. Heat Exchanger Design Handbook, vol. 2. Hemisphere, New York, pp. 235–251.

Inasaka, F., Nariai, H., Shimura, T., 1989. Pressure drops in subcooled flow boiling in narrow tubes. Heat Transfer Japanese Research 18, 70–82.

John, H., Reimann, J., Westphal, F., Friedel, L., 1988. Critical two-phase flow through rough slits. Int. J. Multiphase Flow 14, 155–174.

Lockhart, R.W., Martinelli, R.C., 1949. Proposed correlation of data for isothermal two-phase, two-component flow in pipes. Chem. Eng. Prog. 45, 39–48.

McAdams, W.H., 1954. Heat Transmission. 3rd ed. McGraw–Hill, New York.

Narabayashi, T., Makoto, F., 1991. Experimental study on leak flow model through fatigue crack in pipe. Nucl. Eng. Design 128, 17–27.

Premoli, A., Francesco, D., Prina, A., 1971. A dimensionless correlation for determining the density of two-phase mixtures. Lo Termotecnica 25, 17–26.

Triplett, K.A., Ghiaasiaan, S.M., Abdel-Khalik, S.I., Sadowski, D.L., 1999. Gas–liquid two-phase flow in microchannels. Part I: two-phase flow patterns. Int. J. Multiphase Flow 25, 377–394.

Ungar, E.K., Cornwell, J.D., 1992. Two-phase pressure drop of ammonia in small diameter horizontal tubes. AIAA 17th Aerospace Ground Testing Conf., Nashville, TN, July 6–8.

Wallis, G.B., 1969. One-dimensional two-Phase Flow. McGraw–Hill, New York.

Yao, G.F., Ghiaasiaan, S.M., 1996. Wall friction in annular-dispersed two-phase flow. Nucl. Eng. Design 163, 149–161.

Zuber, N., Findlay, J., 1965. Average volumetric concentration in two-phase flow systems. J. Heat Transfer 87, 453–468.